

Supporting Information

Oxygen-iron interaction in liquid lead-bismuth eutectic alloy

A. Aerts,^{*a} S. Gavrilov,^b G. Manfredi,^a A. Marino,^a K. Rosseel^a and J. Lim^a

THERMODYNAMIC DERIVATION OF THE MAGNETITE SOLUBILITY PRODUCT

The dissolution/precipitation of magnetite is assumed to follow the following reaction:



This reaction has an equilibrium constant/solubility product:

$$K_{sp}^* = a_{\text{Fe}(\text{lbe})}^3 a_{\text{O}(\text{lbe})}^4 \quad (2)$$

where the factors a are the activities of dissolved iron and dissolved oxygen in LBE. Alternatively, the solubility product can be expressed in terms of dissolved concentrations C , where typically wt% units are used (this involves a change of the standard state of the dissolved metal and oxygen atoms from pure phase standard state to a Henry's law standard state):

$$K_{sp} = C_{\text{Fe}(\text{lbe})}^3 C_{\text{O}(\text{lbe})}^4 \quad (3)$$

The free energy change of reaction (1) is:

$$\Delta_r G^\circ = \Delta_f G_{\text{Fe}_3\text{O}_4(\text{s})}^\circ - 3\Delta_f G_{\text{Fe}(\text{lbe})}^\circ - 4\Delta_f G_{\text{O}(\text{lbe})}^\circ \quad (4)$$

Using the well-known relation between Gibbs free energy and equilibrium constant, the solubility product can be derived from the following data:

The Sieverts constant of oxygen dissolution in LBE is (1 wt% standard state for dissolved oxygen; 1 bar for $\text{O}_2(\text{g})$) [Lim2015]:

$$\log k = 3.12 - \frac{7072}{T} \quad (5)$$

The excess Gibbs free energy [kJ/mol] for dissolved oxygen in LBE can then be calculated:

$$\Delta_f G_{O(lbe)}^\circ = RT \ln k = -135.32 + 0.0597T \quad (6)$$

The solubility of iron metal in LBE is (1 wt% standard state) [Gossé2014]:

$$\log C_{Fe(lbe)} = 2.01 - \frac{4398.6}{T} \quad (7)$$

The excess Gibbs free energy [kJ/mol] for dissolved iron in LBE is calculated from the solubility by:

$$\Delta_f G_{Fe(lbe)}^\circ = -RT \ln C_{Fe(lbe)} = 84.16 - 0.03846T \quad (8)$$

The free energy of formation of magnetite is taken from tabulated values in [Barin1995] (Table si-1).

Table si-1. Free energy of formation of magnetite [Barin1995]

T	$\Delta_f G_{Fe_3O_4(s)}^\circ$
K	kJ/mol
298.15	-1015.227
300	-1014.587
400	-980.368
500	-946.969
600	-914.396
700	-882.629
800	-851.723
850	-836.656

The values in table SI-1 can be correlated as:

$$\Delta_f G_{Fe_3O_4(s)}^\circ = -1111 + 0.3245T \quad (9)$$

Inserting Eqs. (6), (8) and (9) in Eq. (4) gives

$$\Delta_r G_{diss, Fe_3O_4}^\circ = 822.0 - 0.2011T \quad (10)$$

for the free energy of reaction of magnetite dissolution in LBE. The corresponding solubility product constant is:

$$\begin{aligned} \log K_{sp} &= \log [C_{Fe(lbe)}^3 C_{O(lbe)}^4] \\ &= 10.5 - \frac{42935}{T} \end{aligned} \quad (11)$$

OXYGEN PUMPING EXPERIMENT

Experimental

Lead-bismuth eutectic (99.99%, 5nplus) was used, which according to NAA and ICP-MS analyses, contained Ag (17 wt-ppm) and Cu (9 wt-ppm) and Ni (7 wt-ppm) as most abundant impurities. The total iron impurity content was less than 0.16 wt-ppm.

Approximately 5500 g of LBE was placed in an alumina crucible that was inserted in a stainless steel pot wrapped with electrical heaters. The alumina crucible was used to avoid chemical interaction between the LBE and the stainless steel container. To improve the heat transfer, LBE was also placed in the gap between the stainless steel pot and the alumina crucible.

The oxygen concentration in LBE was measured by an oxygen sensor with of yttria partially stabilized zirconia (YPSZ) solid electrolyte and Bi/Bi₂O₃ reference electrode described elsewhere [Lim2012].

The temperature was monitored using a K-type thermocouple with SS304 sheath immersed in LBE. The thermocouple sheath, in contact with LBE, was connected to the ground and used as electrical lead wire for the working electrode (LBE).

The potential difference between reference and working electrodes was measured by an Agilent 34972A voltmeter, selecting a high input resistance (> 10 GΩ) and 200 NPLC (number of power line cycles). These settings were chosen to reduce the noise uptake from the environment in which the test was performed.

Next to the oxygen sensor, an oxygen pump was placed into the LBE. The oxygen pump was fabricated using yttria partially stabilized zirconia as a solid electrolyte and LSM (strontium-doped lanthanum manganite)–GDC(gadolinium-doped ceria) composite as a cathode. The oxygen pump was connected to a DC current source which was regulated by a PID controller (Invensys Eurotherm, 3216 process controller). The electric potential difference measured by the oxygen sensor was used as a control value for the PID controller. The details of the oxygen pump system can be found in ref. [Lim2014].

Results and simulation

In this experiment, oxygen was added by electrochemical oxygen pumping to an autoclave filled with LBE at 500 °C and the concentration of dissolved oxygen was measured concurrently (Fig. si-1).

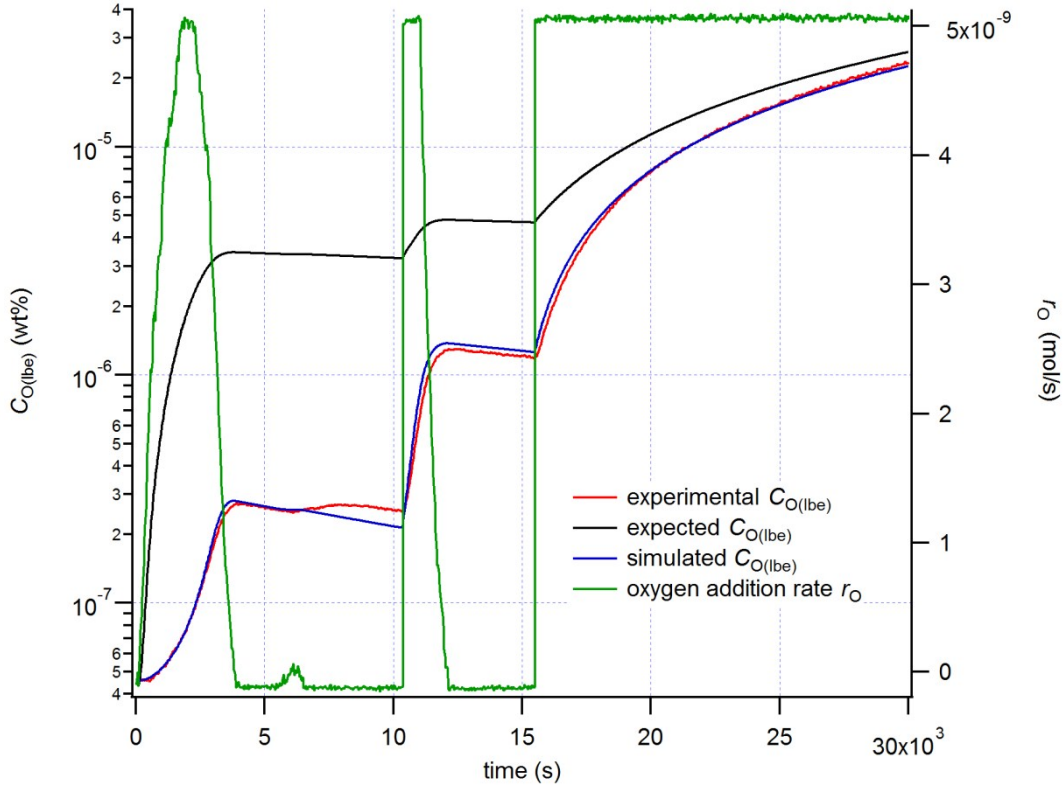


Figure si-1. Oxygen pumping experiment: data and simulation.

To model the measured oxygen concentration trend, the following differential equation was derived from the oxygen mass balance in the system and the solubility product:

$$\frac{dC_{O(lbe)}}{dt} = \frac{r_O(t)}{0.01m_{lbe} \left(1 + \frac{16}{9} \frac{M_O}{M_{Fe}} K^{1/3} C_{O(lbe)}^{-7/3} \right)} \quad (\text{si-12})$$

where M is the molar mass and m_{LBE} is the total mass of the LBE in the experiment. The factor $r_O(t)$ is the time-dependent net oxygen addition rate. The net oxygen addition rate was calculated as the electrochemical pumping rate minus a small and constant oxygen consumption rate by the system (i.e. by steel surfaces exposed to LBE). The latter was derived from the change of oxygen concentration while the electrochemical pump current was zero and amounted to -1.2×10^{-10} mol/s O.

The differential equation Eq. si-12 was integrated and fitted to the experimental data by a home made Python code, taking into account the applied $r_O(t)$ and the initially measured oxygen concentration. The solubility product constant was the only fit parameter. Best fit was found for $\log K_{sp} = -44.48$, whereas the correlation (Eq.si-11 and Eq.2) predicts $\log K_{sp} = -45.03$.

CALCULATION OF ISO-COMPOSITION LINES IN THE (Pb,Bi)-Fe-O PHASE DIAGRAM

Constant composition lines in the (Pb,Bi)-Fe-O phase diagram were calculated by solving the following differential equation, derived from the oxygen mass balance in the system and the solubility product:

$$\frac{dC_{O(\text{lbe})}}{dT} = \frac{C_{O(\text{lbe})} \frac{dK}{dT}}{\frac{9}{4} \frac{M_{\text{Fe}}}{M_{\text{O}}} C_{O(\text{lbe})}^{7/3} K^{2/3} + 4K} \quad (\text{si-13})$$

where K is again the magnetite solubility product.

TEMPERATURE CYCLING EXPERIMENT

Experimental

In a stainless steel autoclave equipped with an oxygen sensor (see above), thermowell and alumina liner, 5500 g of lead-bismuth eutectic (99.99%, 5nplus) was placed. The autoclave was closed, and the temperature was increased to 500 °C. Before the temperature cycling, the oxygen concentration in the LBE was decreased to below 10⁻⁷ wt% by flowing Ar/5%H₂. After reduction, the cover gas was changed to 10 mL/min of high purity Ar (BIP®, Air Products) and the temperature was cycled between 500 °C and 300 °C at a rate of 1.6 °C/min.

Simulation

The oxygen concentration measurement during the temperature cycling experiment was simulated by solving the following differential equation, derived from the oxygen mass balance in the system and the solubility product:

$$\frac{dC_{O(\text{lbe})}}{dt} = \frac{r_l + 0.01m_{\text{lbe}} \frac{4M_{\text{O}}}{9M_{\text{Fe}}} C_{O(\text{lbe})}^{-4/3} K^{-2/3} \frac{dK}{dt}}{0.01m_{\text{lbe}} \left(1 + \frac{16M_{\text{O}}}{9M_{\text{Fe}}} K^{1/3} C_{O(\text{lbe})}^{-7/3} \right)} \quad (\text{si-14})$$

where r_l is a constant oxygen inleak rate. The differential equation was solved numerically using the applied temperature cycling profile as input. The experimental temperature profile was synthesized using the 7 first terms of the Fourier series of a triangular wave. This way discontinuities (from the noise on the experimental data) were avoided and analytical expressions for $K(t)$ and dK/dt for evaluation of Eq. (si-14) could be derived. The resulting $C_{O(\text{lbe})}$ versus time for $r_l = 1.7 \times 10^{-11}$ wt% s⁻¹ in 5500 g LBE starting from $C_{O(\text{lbe})} = 5.6 \times 10^{-8}$ wt% is shown in Figure si-2. Figure 3 of the manuscript depicts $C_{O(\text{lbe})}$ versus temperature.

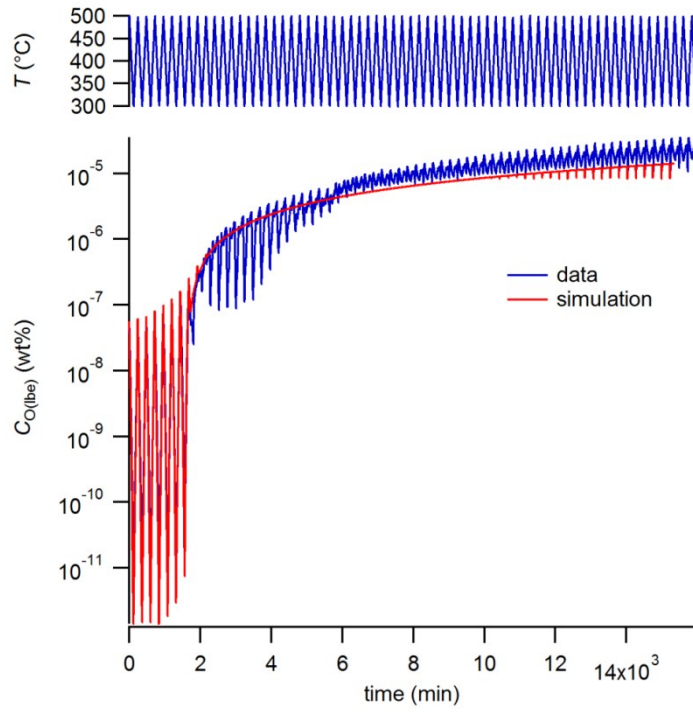


Figure si-2. Temperature cycling experiment. (bottom) Measured oxygen concentration and simulation; (top) corresponding temperature profile.

CHARACTERIZATION OF PRECIPITATES FROM THE CRAFT LOOP

Experimental

Powder X-ray diffraction patterns were recorded on a Philips X'pert Pro diffractometer using Cu K α radiation. Scanning Electron Microscopy images were recorded on a JEOL JSM6610 LV instrument. Energy-dispersive X-ray spectrometry (EDX) was performed using a Quantax instrument by Bruker Nano GmbH.

Results

A picture of slag extracted from the CRAFT loop is shown in Fig. Si-3. XRD showed that the major phases in the slag were the LBE constituent phases Bi and Pb₇Bi₃, PbO and a significant amount of magnetite (Fig. Si-4). A secondary electron SEM image and corresponding EDX analysis revealed that the slag consisted of micron sized iron-rich particles in a (Pb,Bi) rich matrix (Fig. Si-5). Magnetite particles were also found in the LBE sticking on the surface of steel specimens that were extracted from the CRAFT loop (Fig. Si-6).



Figure si-3. Picture of slag accumulated at the free surface between LBE and argon cover gas of the sample extraction point in the CRAFT loop.

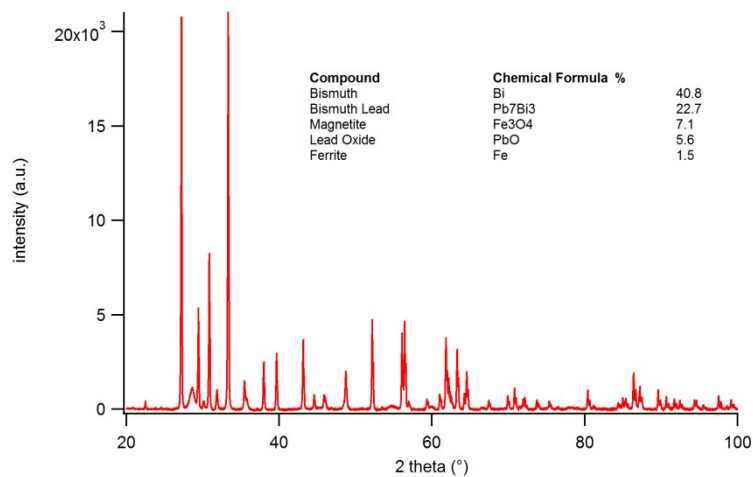


Figure si-4. XRD pattern of the slag and estimated composition.

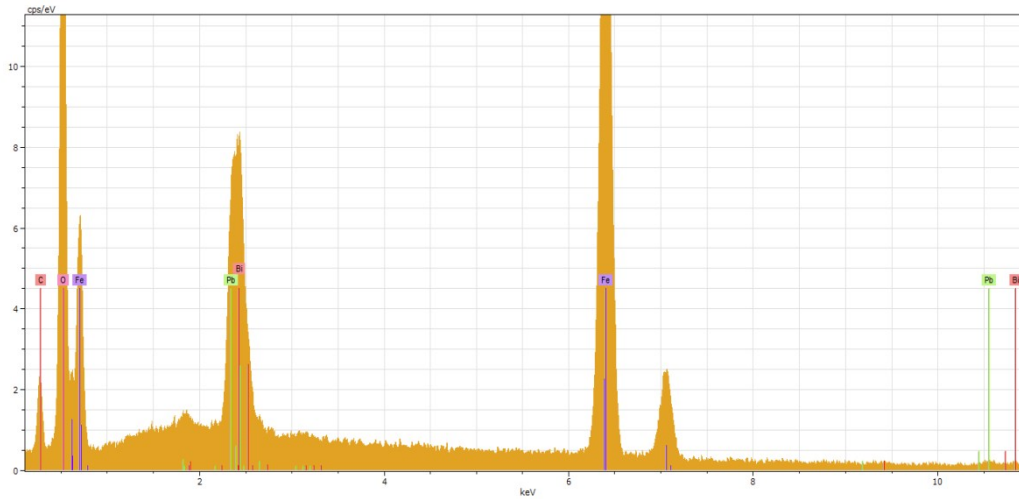
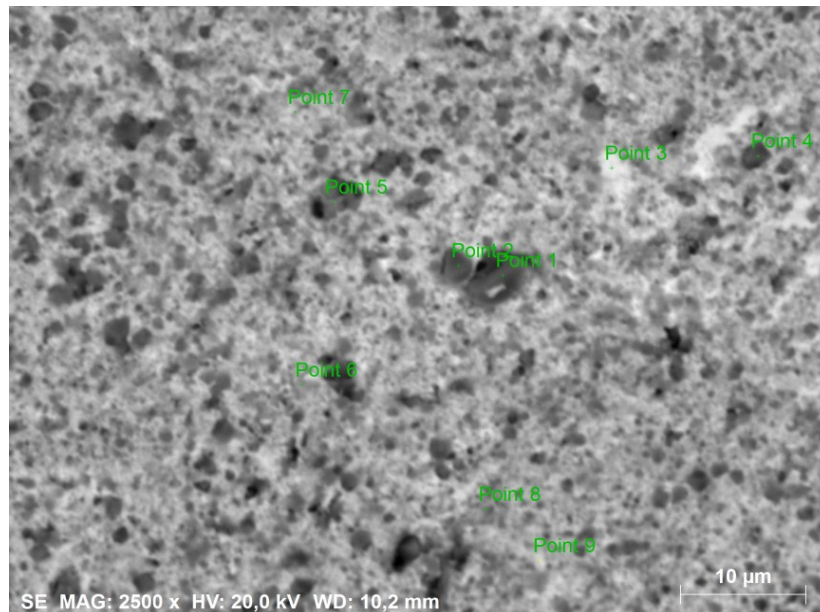


Figure si-5. (top) Secondary electron SEM image of slag. (bottom) EDX of a dark contrast particle in the SEM image (point 4) revealed that these were enriched in iron compared to the areas with lighter contrast.

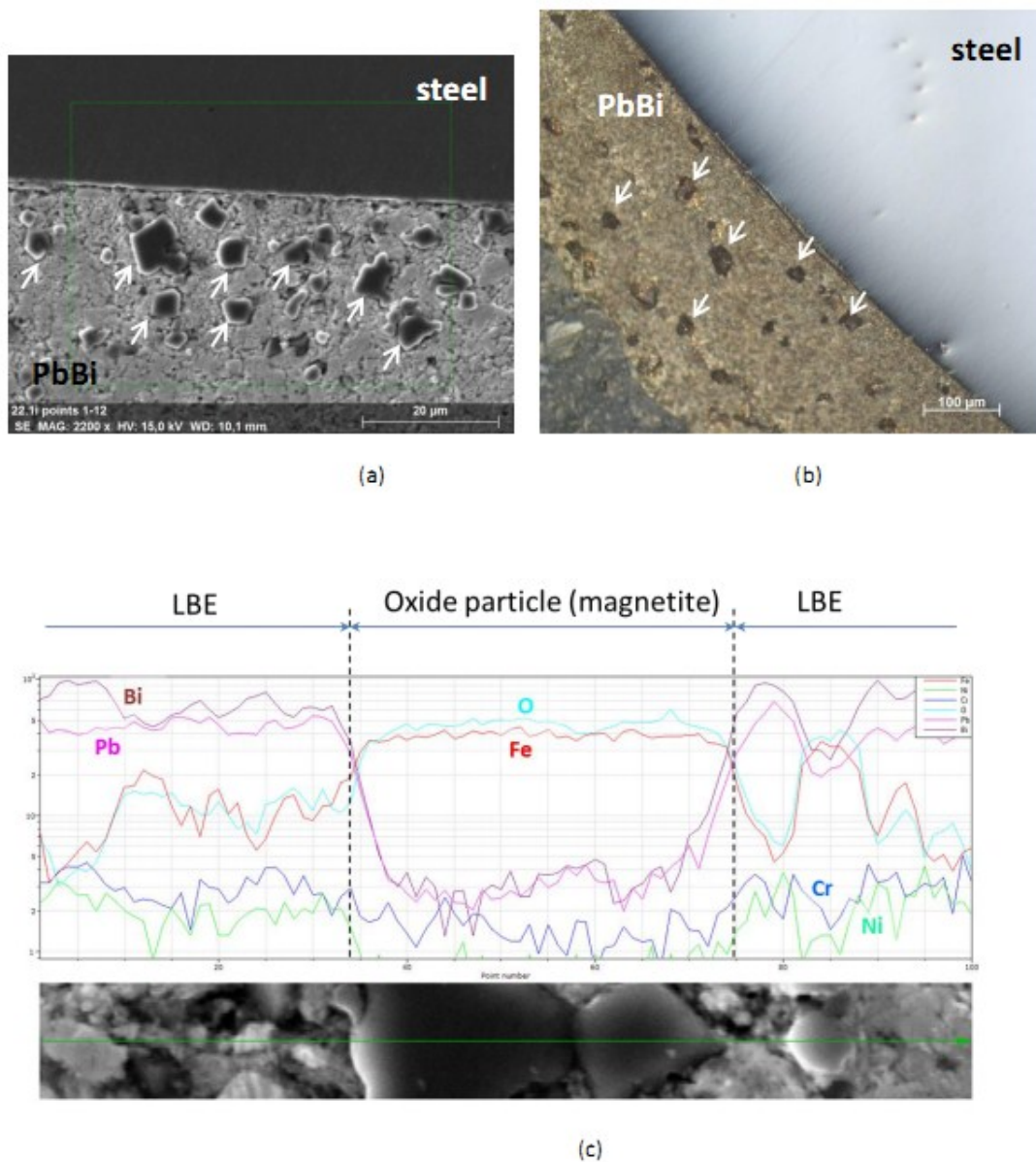


Figure si-6. Magnetite particles in LBE adjacent to the steel surface indicated with arrows (a: SEM image of a steel specimen section; b: optical image). Typical elemental profile of magnetite particle and surrounding LBE (c)

REFERENCES

[Barin1995] I. Barin, Thermochemical Data of Pure Substances Wiley, 1995.

[Gosse2014] S. Gossé, Thermodynamic assessment of solubility and activity of iron, chromium, and nickel in lead bismuth eutectic *Journal of Nuclear Materials*, 2014, **449**, 122-131.

[Lim2012] J. Lim, A. Marien, K. Rosseel, A. Aerts and J. Van den Bosch Accuracy of potentiometric oxygen sensors with Bi/Bi₂O₃ reference electrode for use in liquid LBE *Journal of Nuclear Materials*, 2012, **429**, 270-275.

[Lim2014] J. Lim, G. Manfredi, S. Gavrilov, K. Rosseel, A. Aerts and J. Van den Bosch, Control of dissolved oxygen in liquid LBE by electrochemical oxygen pumping *Sensors and Actuators B-chemical*, 2014, **204**, 388-392.